Chapter 7

Thermo-Shrinkable Elastomers

Magdalena Maciejewska and Alicja Krzywania-Kaliszewska

Additional information is available at the end of the chapter

http://dx.doi.org/10.5772/48209

1. Introduction

The ability of polymeric materials to sense and respond to external stimuli has great scientific and technological significance. It enables these materials to change their properties, such as shape, colour and electrical conductivity, as a result of pH, temperature, chemicals, light, or stimulation by an electric or magnetic field. Materials that respond dynamically to external stimuli are called intelligent or smart materials, and it is important that their response should be repeatable and controllable (Landlein, 2010). One of the most important classes of smart materials is shape memory polymers (SMPs), which can change their shape in a predetermined way upon the application of an external stimulus. The shape memory effect in polymers depends primarily on the existence of separated phases that are related to the coiled structure, crosslinks (covalent bonds), hydrogen or ionic bonding or physical intermolecular interactions of the polymer (Hu, 2007). Covalent crosslinks are formed during suitable crosslinking of the polymer, whereas physical crosslinks are obtained when the polymer morphology consists of segregated domains, such as crystalline and amorphous phases or hard and soft segments (Landlein, 2010) (e.g., linear block copolymers). In multiphase polymers, the hard segments act as the frozen phase, which is usually semi-crystalline or physically crosslinked and provides stiffness and reinforcement to the material (Hu, 2007), while the soft segments are responsible for the thermo-elastic behaviour of polymers and act as the reversible phase. In this case, the shape memory effect is produced by the reversible phase transformation of the soft segments (Hu, 2007). Thermo-shrinkable polymers, which change their shape as the temperature changes, are a unique class of SMP materials with interesting properties and many potential applications. The shape transition temperature (T_{trans}) for this type of SMP can be the melting point (T_m) or glass transition temperature (T_g) of the soft phase (Ratna & Karger-Kocsis, 2008). Melting points are preferred because the transition is sharper than the glass transition; therefore, the temperature of the shape recovery can be better determined. Heating the SMP above the T_m or T_g of the hard segment enables its processing. This original (permanent) shape can be

memorised by cooling the material below the T_m or T_g of the hard phase. Cooling the SMP below the T_m or T_g of the soft segment while the shape is deformed allows a temporary shape to be fixed. The permanent shape of the SMP is recovered by heating it above the T_m or T_g of the soft phase (Hu, 2007). Another way to fix the temporary shape of a SMP is to deform it at a temperature lower than the T_m or T_g of the soft phase, which causes stress and strain absorption by the soft segments. When the material is heated above the T_m or T_g of the soft segments, the stresses and strains are relieved, causing the material to return to its original shape (Leng & Du, 2010). The thermally induced shape memory effect in polymers is schematically presented in Figure 1. SMPs that use T_m as the shape transition temperature are represented by polymers such as polyurethanes, block copolymers of polyethyleneterephthalate and polyethyleneoxide, and copolymers consisting of polystyrene and poly(1,4-butadiene) (Wang et al., 1998). T_g is the shape transition temperature for thermoset SMPs; e.g., styrene-based resins (Ivens et al., 2011). SMPs can also be single phase materials with a certain number of crosslinks between their polymer chains. In this case, the crosslinks are the net points that enable fixing and storage of the permanent shape of the polymer, whereas the free polymer chains between the crosslinks act as switching segments that possess increased mobility above T_g (Ratna & Karger-Kocsis, 2008). Stretching the polymer chain segments in a certain direction reduces their entropy. At the same time, the net points deform elastically. The overall result of this process is an increase in the SMP enthalpy. The loss of polymer chain segment mobility in the switching segments stabilises the temporary shape of the SMP when the material is allowed to cool in the deformed state (Ivens et al., 2011).

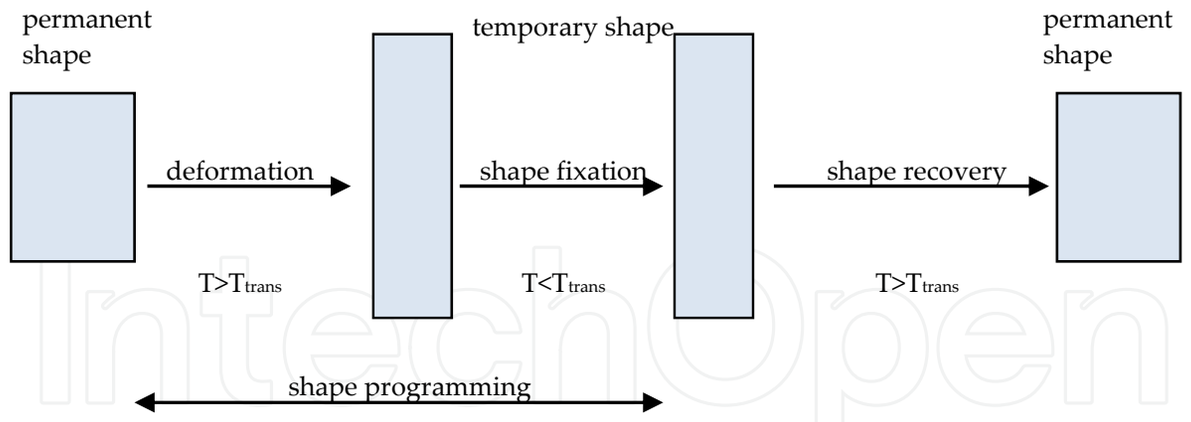

Figure 1. Thermally induced shape memory effect in polymers

Recently, research activities related to the development of elastomeric composites that exhibit a thermally induced shape memory effect have intensified. Thermoplastic elastomers (TPEs) are an interesting class of materials. TPEs behave like cured elastomers at room temperature, and they can be processed as plastics at higher temperatures because of their special multiphase morphology. TPEs consist of plastic phases embedded in a continuous elastomer phase, and they form physical crosslinks. Among the TPEs, segmented polyurethane elastomers and ionomers or blends of elastomers with thermoplastic polymers

have many potential applications. In shape memory polyurethanes, the hard segment phases with the highest thermal transition temperatures (T_{perm}) acts as the physical crosslink points and control the permanent shape of the polymer. When the polymer is heated above T_{perm}, the physical crosslinks between the hard segments are destroyed. The molecular chains melt, and the polymer can be processed to a permanent shape like a thermoplastic material. When the shape memory polyurethane is cooled below T_{perm} and above T_g or T_m of its soft segments, the polymer becomes relatively soft, but it cannot flow because of the physical crosslinks. Consequently, it can be easily deformed to a temporary shape by stretching or compression. Reheating the polymer above T_g or T_m of its soft segments but below T_{perm} induces shape recovery (Hu, 2007). In the case of polyolefin/elastomer blends, the crosslinked elastomeric phase causes an enhancement of the blend shrinkability upon heating. Crosslinked points in the elastomer network are believed to serve as memory points, increasing the heat shrinkability (Patra & Das, 1997). Weiss et al. designed a new type of SMP based on blends of an elastomeric ionomer and low molar mass fatty acids or their salts (Weiss et al., 2008). Nanophase separation of the ionomer was used to develop the permanent network, and the fatty acids or salts were used to produce a secondary network. The role of the ionomer was to provide a strong intermolecular bond between crystals of the fatty acids or salts and the polymer, acting as a physical crosslink below the fatty acids or salt T_m and allowing reshaping of the material above T_m. The polymer films were heated to 100°C and stretched to 47% strain, then cooled to room temperature to fix an elongated temporary shape. When the samples were reheated to 100°C, the film recovered to the permanent shape with a length recovery of approximately 92%. A two-way temperature-induced shape memory effect was observed for polymer laminates. SMP-laminated composites were prepared with SMP polyurethane films and elastic polymers films. Their two-way shape memory behaviour was produced by bending upon heating and reverse bending upon cooling. The shape memory mechanism was ascribed to the release of the elastic strain of the SMP layer upon heating and the recovery of the elastic strain induced by the bending force of the substrate layer upon cooling (Chen et al., 2008). Mishra et al. have studied the heat shrinkability behaviour of grafted low-density polyethylene/polyurethane elastomers. They have suggested that the interchain crosslinking between the grafted polyethylene and the elastomer improves their shrinkability (Mishra et al., 2004).

Zhang et al. reported a novel type of shape memory polymer blend that consisted of two immiscible components, an elastomer and a switch polymer. The elastomer could be a rubber or thermoplastic elastomer, and the switch polymer could be an amorphous or crystalline polymer. Styrene–butadiene–styrene tri-block copolymer (SBS) was chosen as the elastomer, and poly(ε-caprolactone) (PCL) was used as the switch polymer (Zhang et al., 2009). The SBS/PCL blends demonstrated good shape recovery performance, with a shape recovery ratio of approximately 100%. The shape memory effect was also observed in elastomer networks containing reversibly associating side-groups. The supramolecular shape-memory elastomer consisted of a lightly crosslinked polymer network that was covalently bonded to reversibly associating side-groups. These elastomers exhibited shape-memory effects arising from reversible hydrogen bond association, and the shape memory

recovery rate was strongly dependent on the temperature. Hydrogen-bonding interactions could stabilise mechanically strained states in these elastomers, and the thermo-mechanical cycling produced a strain fixity of approximately 90% and a strain recovery of approximately 100% (Li et al., 2007).

Thermal shrinkability was also reported for elastomer blends containing carboxylated groups, which could form ionic labile bonds during crosslinking, and low-density polyethylene (Mishra et al., 2000) or poly(ethylene-vinyl-acetate) (Raychowdhury et al., 2000).

In our previous studies, we proved that the thermally induced shape memory effect was also exhibited by a carboxylated nitrile elastomer cured with zinc oxide because it contained labile ionic crosslinks, which were able to rearrange upon external deformation (Przybyszewska & Zaborski, 2009).

In this work, the thermo-shrinkable properties of carboxylated acrylonitrile – butadiene elastomer (XNBR) and hydrogenated acrylonitrile – butadiene elastomer (HNBR) containing ionic crosslinks were studied. The XNBR was vulcanised with nanosized calcium, magnesium oxide or zinc oxide to ensure the formation of ionic crosslinks during vulcanisation. In the case of HNBR, nanosized calcium and magnesium oxides were coated with unsaturated carboxylic acids (itaconic, 2,4-pentadienoic, oleic, linoleic and linolenic acids) and applied as coagents in the peroxide vulcanisation of the elastomer. The application of these coagents led to formation of ionic crosslinks in the elastomer network.

Heat-shrinkable polymers are widely used in packaging and in the cable industry; therefore, the shrinkability of XNBR and HNBR vulcanisates is technologically important.

2. Experimental section

2.1. Materials

Carboxylated nitrile elastomer XNBR (Krynac X7.50) containing 27 wt % acrylonitrile and 6.7 wt % carboxylic groups was obtained from Bayer C.O. The Mooney viscosity was (ML1+4 (100^{o}C):47). Nanosized calcium oxide CaO (Aldrich), magnesium oxide MgO (Nanostructured & Amorphous Materials Inc., Houston, USA) and zinc oxide ZnO (Nanostructured & Amorphous Materials Inc., Houston, USA) were used as crosslinking agents. Hydrogenated acrylonitrile-butadiene elastomer HNBR (Therban 3407) containing 34 wt % acrylonitrile and 0.9 wt % of residual double bonds after hydrogenation was obtained from Bayer C.O. The Mooney viscosity was (ML1+4 (100^{o}C):70). It was vulcanised with dicumyl peroxide DCP (Aldrich). Nanosized calcium oxide (Aldrich), magnesium oxide (Nanostructured & Amorphous Materials Inc., Houston, USA), itaconic acid IA (Fluka), 2-4-pentadienoic acid (Aldrich), oleic acid, linoleic acid and linolenic acid (Aldrich) were applied as coagents.

2.2. Preparation of coagents

The nanosized metal oxides were mixed with a solution of modifying agent (unsaturated carboxylic acid) in acetone for 30 minutes during ultrasonic treatment (BANDELIN DT 255)

at a frequency of 35 kHz. The mixture was left for 24 hours. Then, the solvent (acetone) was evaporated using a vacuum evaporator at 50°C. The coagents obtained were dried in a vacuum drier at 70°C for 96 hours.

2.3. Preparation and characterisation of rubber compounds

Rubber compounds with the formulations given in Table 1 were prepared using a laboratory two-roll mill. The samples were cured at 160°C until they developed a 90% increase in torque, as measured by an oscillating disc rheometer.

The crosslink densities (ν_T) of the vulcanisates were determined by their equilibrium swelling in toluene, based on the Flory-Rehner equation (Flory & Rehner, 1943). The Huggins parameter of the XNBR-solvent interaction (χ) was calculated from the equation $\chi = 0.487 + 0.228V_r$ (Equation 1) (Przybyszewska & Zaborski, 2008), where V_r is the volume fraction of elastomer in the swollen gel, and $\chi = 0.501 + 0.273V_r$ for HNBR-solvent interaction (Equation 2) (Przybyszewska & Zaborski, 2009). To determine the content of ionic crosslinks in the elastomer network, samples were swollen in toluene in a dessicator with saturated ammonia vapour (25% aqueous solution). The ionic crosslink content ($\Delta\nu$) was calculated from Equation 3, where ν_A is the crosslink density determined for samples treated with ammonia vapour.

$$\Delta\nu = \frac{\nu_T - \nu_A}{\nu_T} \bullet 100\% \tag{3}$$

The tensile properties of the vulcanisates were determined according to ISO-37 with a ZWICK 1435 universal machine.

XNBR		HNBR	
Elastomer	100	Elastomer	100
Nanosized metal oxide	4	DCP	2
		Coagent	7

Table 1. Composition of the XNBR and HNBR-based rubber compounds [phr]

2.4. Dynamic-mechanical analysis

Dynamic - mechanical measurements were carried out in the tension mode using a DMA/SDTA861^e analyser (Mettler Toledo). Measurements of the dynamic moduli were performed over the temperature range (-60 - 120°C) for XNBR and (-80 - 100°C) for HNBR with a heating rate of 2°C/min, a frequency of 1 Hz and a strain amplitude of 4 μm. The temperature of the elastomer glass transition was determined from the maximum of $\tan\delta = f(T)$, where $\tan\delta$ is the loss factor and T is the measurement temperature.

2.5. Shrinkability measurements

To measure the shrinkability of the XNBR and HNBR vulcanisates, the samples were stretched above their T_g at a temperature of 100°C until they reached an elongation of 200%

and left in the stretched form for 48 h. They were then stabilised in the stretched form for 4 h at (-7°C). Finally, the stretched samples were allowed to shrink above the ionic transition temperature at 70°C for 48 h. The length of the samples at each state of study was measured using the digital callipers (Preisser) with the measurement error 1 mm. The lengthwise shrinkage was calculated according to Equation 4, in which S_h is the percentage of shrinkability, L_{str} is the length of the sample after stretching, and L_{shr} is the length of the shrunk sample. The maximum shrinkage, S_{hmax}, was calculated from the length of the sample before stretching according to Equation 5, in which L_0 is the original length of the sample before stretching. The physical properties of the vulcanisates were studied before and after the thermal treatment.

$$S_h\% = \frac{L_{str} - L_{shr}}{L_{str}} \bullet 100 \tag{4}$$

$$S_{h\max}\% = \frac{L_{str} - L_0}{L_{str}} \bullet 100 \tag{5}$$

The continuous increase in temperature causes the recovery of the stretched sample deformation, which reflects the memory effect of the vulcanisate. The percentage recovery R is the ratio of the lengthwise shrinkage to the maximum shrinkage (Equation 6) (Khonakdar et al., 2007).

$$R\% = \frac{S_h}{S_{h\max}} \bullet 100 \tag{6}$$

2.6. Scanning Electron Microscopy (SEM)

The morphology of the metal oxide particles and their dispersion in the elastomer matrix were estimated using scanning electron microscopy with a LEO 1530 SEM. The vulcanisates were broken down in liquid nitrogen, and the surfaces of the vulcanisate fractures were examined. Prior to the measurements, the samples were coated with carbon.

3. Results and discussion

3.1. Thermo-shrinkable XNBR vulcanisates

3.1.1. Crosslink density and ionic crosslink content of XNBR vulcanisates

The carboxylated nitrile elastomer XNBR reacts with metal oxides to form carboxylic salts, which behave as ionic crosslinks. These salts are able to associate, forming multiplets and clusters. This association is caused by the electrostatic interactions between multiplets, and it is impaired by the retractive elastic forces of the backbone chains. The restricted elastomer chain mobility in the proximity of the ionic clusters produces a hard phase surrounded with the soft elastomer matrix (Mishra et al., 2000). The biphasic structure of the XNBR

crosslinked with metal oxide and the presence of labile ionic crosslinks provide possible routes to obtain thermo-shrinkable composites.

Because the ionic crosslinks play a crucial role in the return of the sample to the original shape and serve as memory points, the crosslink density and ionic crosslinks content in the elastomer network were determined in the first stage of the study. These results are presented in Figs. 2 and 3.

The nanosized calcium, magnesium and zinc oxides exhibited high crosslinking activity in XNBR. Their application led to the formation of ionic crosslinks in the elastomer network. The content of ionic crosslinks was in the range of 55% to 76%. Nanosized zinc oxide, for which the highest vulcanisate crosslink density and ionic crosslink content was observed (approximately 76%), appeared to be the most active, whereas the lowest activity was exhibited by CaO (with an ionic crosslink content of approximately 55%). Therefore, it could be supposed that the highest shape recovery would be obtained for vulcanisates crosslinked with nanosized ZnO.

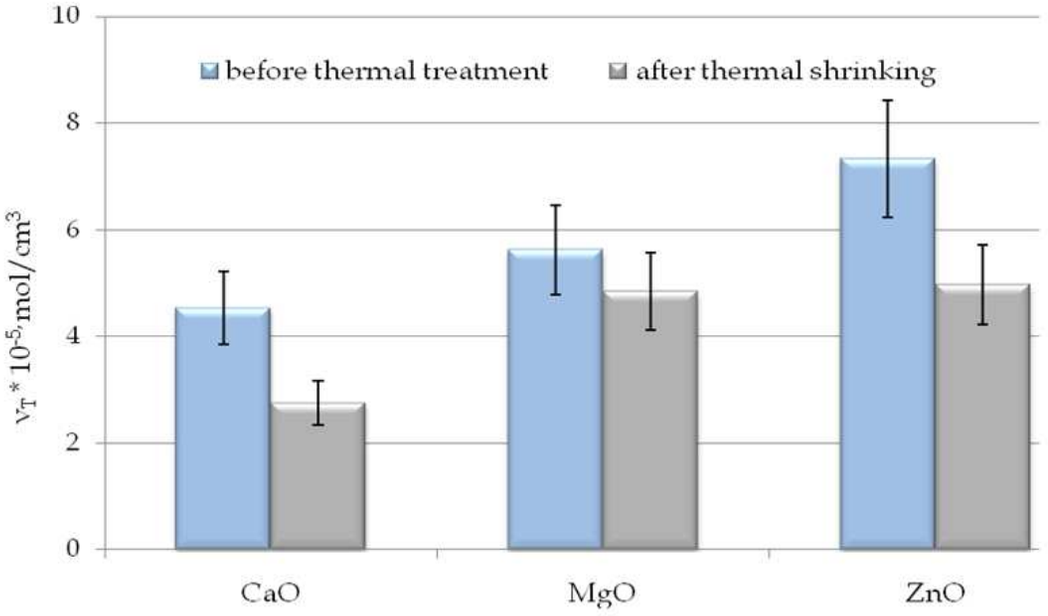

Figure 2. Crosslink density of XNBR vulcanisates

The stretched samples were allowed to shrink above the ionic transition temperature at 70°C to initiate their return to the original shape. The influence of this thermal treatment on the ionic crosslink content and crosslink density of the vulcanisates was studied. From the data presented in Fig. 3, it follows that heating the samples to 70°C caused decomposition of the ionic crosslinks. The number of ionic crosslinks in the elastomer network was reduced by 21-34% compared to the vulcanisates before thermal treatment. The greatest number of ionic crosslinks was decomposed in the case of vulcanisates containing nanosized ZnO.

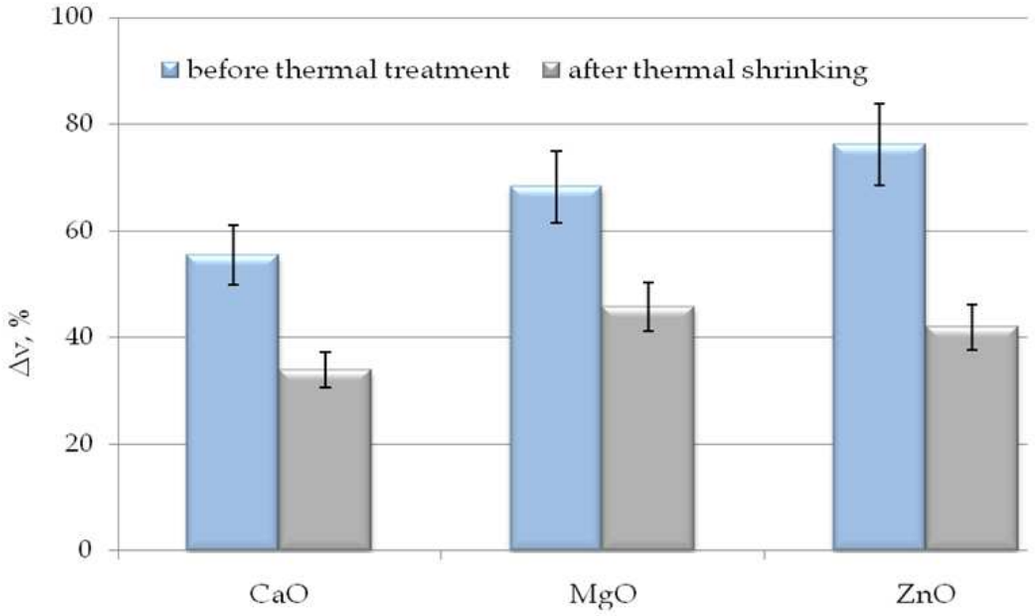

Figure 3. Ionic crosslink content in XNBR vulcanisates

3.1.2. Thermo-shrinkability of XNBR vulcanisates

Having determined the number of ionic crosslinks in the elastomer network and confirmed that these crosslinks could decompose during thermal treatment, we then examined the thermo-shrinkability of the vulcanisates. In Fig. 4, the percentage of thermo-shrinkability and the percentage shape recovery of the vulcanisates are presented.

The vulcanisates of XNBR crosslinked with nanosized calcium, magnesium and zinc oxides exhibited heat shrinkability. The greatest shrinkage upon heating (50%) was achieved for vulcanisates containing ZnO nanoparticles. The lower shrinkability of the vulcanisates with calcium and magnesium oxides (42% and 41%, respectively) was produced by the lower crosslink density and ionic crosslink content in their elastomer networks. Because the crosslinked points in the elastomer network serve as shape memory sites, a greater crosslink density improves the shrinkability of the XNBR. The vulcanisates demonstrated good shape recovery performance. The percentage shape recovery was in the range of 90-100% (Fig. 4). The highest percentage recovery was observed for vulcanisates containing ZnO, which had the greatest ionic crosslink content. The stretched XNBR samples shrunk upon heating above the temperature of the ionic transition because of the occurrence of ionic clusters in the elastomer network, which could rearrange or decompose. The results described in the previous section confirm that the decomposition of the ionic crosslinks is one of the reasons for the heat shrinkability of the XNBR vulcanisates containing nanosized CaO, MgO and ZnO.

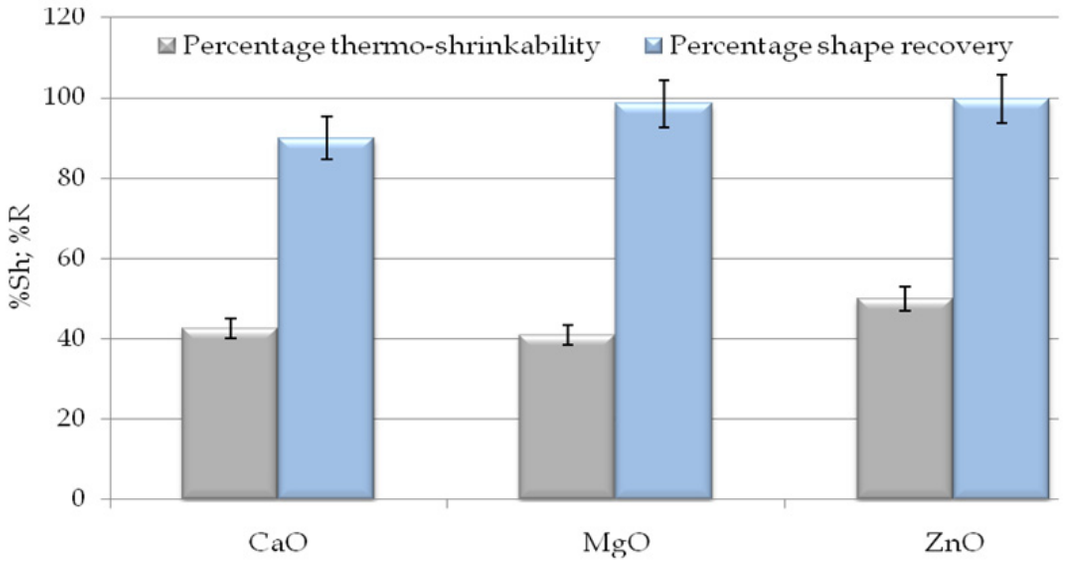

Figure 4. Percentage thermo-shrinkability and shape recovery of XNBR vulcanisates

3.1.3. Dynamic mechanical properties of XNBR vulcanisates

Dynamic - mechanical analysis was performed to confirm the biphasic structure of XNBR crosslinked with nanosized metal oxides, as well as the existence of ionic clusters in the elastomer network. The values of the glass transition temperature (T_g) are given in Table 2. The loss factor, tanδ, is presented in Fig. 5 as a function of temperature for the vulcanisates before thermal treatment.

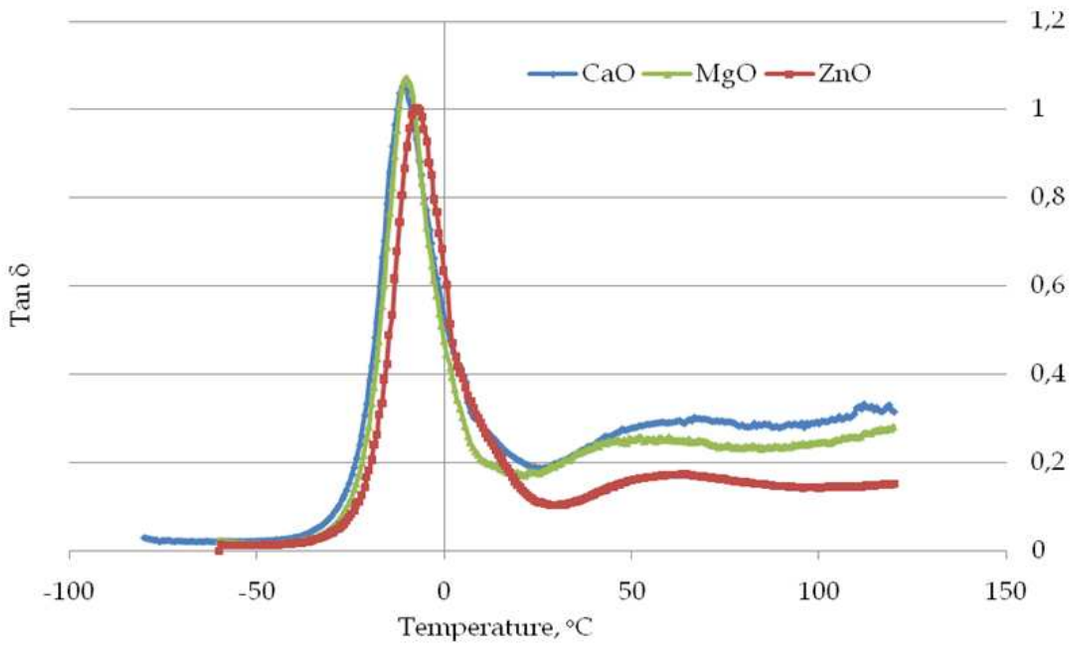

Figure 5. Tan δ versus temperature for XNBR vulcanisates before thermal treatment

The results of the DMA analysis confirm the biphasic structure of the XNBR crosslinked with nanosized CaO, MgO and ZnO. The existence of two phase transitions was observed. The first transition is the glass transition of the XNBR at low temperatures, the maximum of which represents T_g. The determined glass transition temperatures for the vulcanisates with MgO and ZnO were approximately (-11.1°C) and (-10.5°C), respectively, whereas the T_g value was (-13.0°C) for the vulcanisate with CaO nanoparticles. The CaO vulcanisate most likely exhibits the lowest T_g because it contains the lowest crosslink density of the vulcanisates. The second peak, which is fuzzy and has a low-intensity, was observed in the temperature range of (50-100°C). This peak corresponds to the ionic transition at high temperature that is caused by the occurrence of a hard phase arising from ionic associations (ionic clusters or aggregates). These transitions were observed for all XNBR vulcanisates. Therefore, the existence of a biphasic structure in XNBR crosslinked with metal oxides was confirmed.

Vulcanisate	T_g before thermal treatment, °C	T_g after thermal shrinking, °C
CaO	-13.0	-15.0
MgO	-11.1	-13.5
ZnO	-10.5	-16.0

Table 2. Glass transition temperature of XNBR vulcanisates

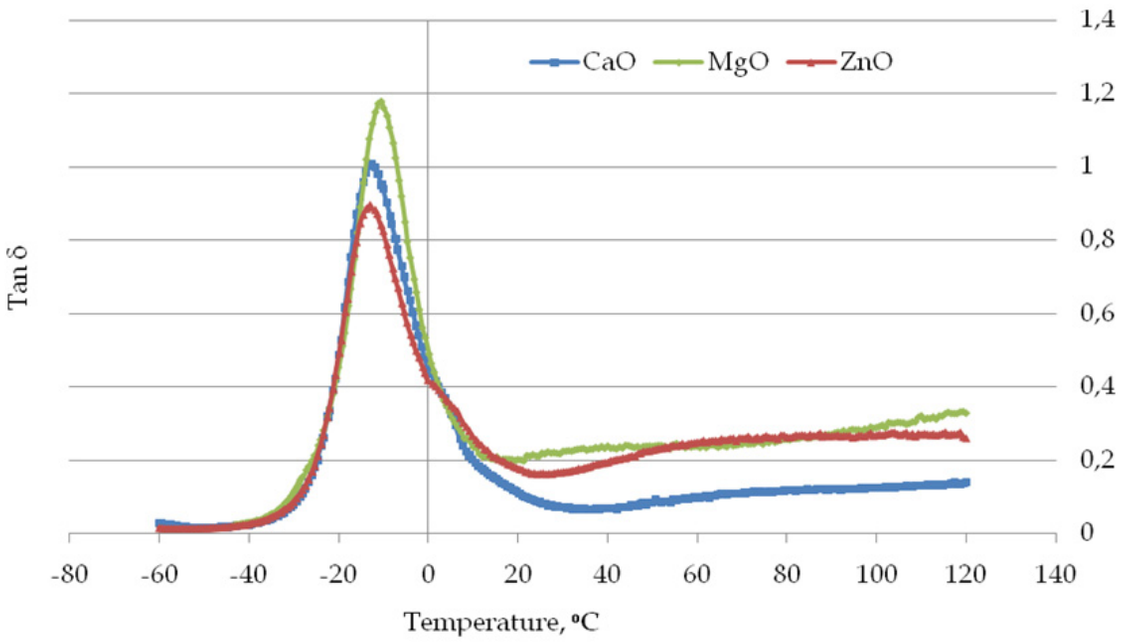

Figure 6. Tan δ versus temperature for XNBR vulcanisates after thermal shrinking

DMA measurements were also performed for the vulcanisates after the thermal shrinking process. These results are presented in Fig. 6. Heating the samples to the ionic transition temperature decreased the glass transition temperatures of the vulcanisates. This reduction was most likely caused by the decomposition of the ionic crosslinks, leading to a reduction of the crosslink density of the vulcanisates. The highest decrease in the T_g value was

observed for the vulcanisate containing nanosized ZnO, for which the greatest amount of ionic crosslinks decomposed during the thermal treatment. The second fuzzy peak corresponding to the ionic transition disappeared, which suggests that the return of the vulcanisates to their original shape was caused by the decomposition of ionic crosslinks, along with changes in or the disappearance of the biphasic structure of the crosslinked elastomer.

3.1.4. Mechanical properties of XNBR vulcanisates

The mechanical properties of the vulcanisates (especially their tensile strength) are technologically important. Therefore, the effect of the thermal shrinking process on the tensile strength and elongation at break of the vulcanisates was studied. These results are presented in Table 3.

Vulcanisate	TS_0, MPa	TS_{shr}, MPa	EB_0, %	EB_{shr}, %
CaO	17.6	12.0	803	734
MgO	37.0	34.4	704	544
ZnO	28.1	20.7	634	525

Table 3. Tensile strength and elongation at break of XNBR vulcanisates before thermal treatment (TS_0, EB_0) and after thermal shrinking (TS_{shr}, EB_{shr})

Regarding the properties of the vulcanisates before the thermal treatment, the greatest tensile strength was exhibited by the vulcanisate with nanosized MgO, whereas the lowest was produced by CaO. One possible reason for the different activities of the metal oxides is their tendency to agglomerate in the elastomers (see Fig. 7).

The CaO nanoparticles were poorly dispersed in the elastomer matrix (Fig. 7a). They created microsized agglomerates with complex structures, which displayed poor adhesion to the elastomer. These agglomerates acted as centres for stress concentration in the vulcanisates during the deformation and initiate breakage of the sample under external stress. As a result, the tensile strength of the vulcanisates decreased. The ZnO nanoparticles also created microsized agglomerates that were smaller than the CaO particles and surrounded by an elastomer film (Fig. 7c). The wetting of the ZnO agglomerates with the elastomer probably produced the better mechanical properties of the ZnO vulcanisates, despite the heterogeneous dispersion of the nanoparticles. The MgO nanoparticles revealed the weakest ability to agglomerate in the XNBR, creating clusters of approximately 3 μm in size that were tightly bound to the elastomer matrix (Fig. 7b). The highest tensile strength was observed for the vulcanisate with MgO. The elongation at break was the lowest for the vulcanisate containing ZnO nanoparticles, and this result was correlated with the crosslink density of the examined vulcanisates.

The stretching of the samples at high temperature, their stabilisation in the stretched state and the shrinkage above the ionic transition temperature reduced the tensile strength and elongation at break of the vulcanisates by decomposing the ionic crosslinks and reducing the crosslink density of the vulcanisates. However, these mechanical properties remained

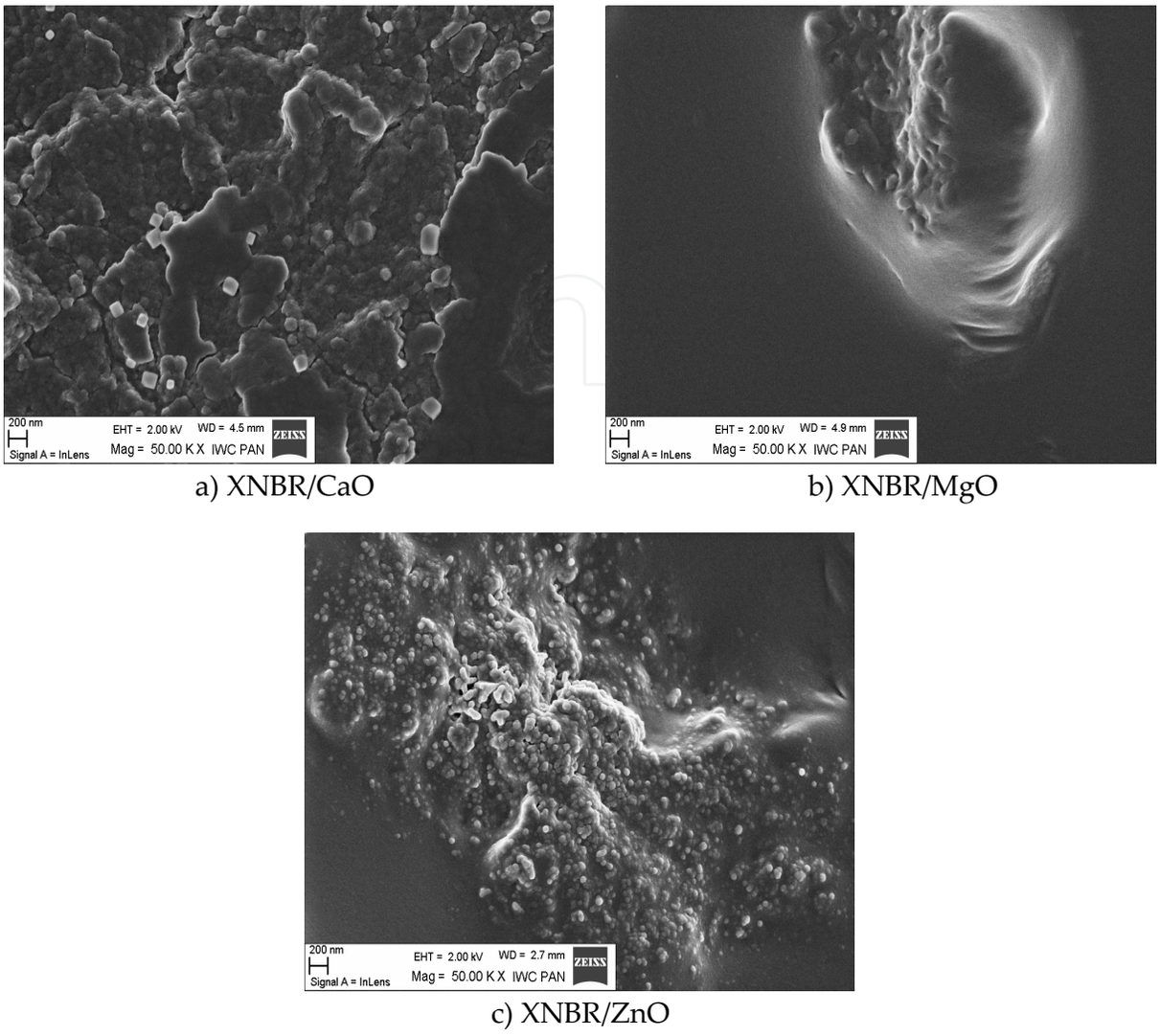

a) XNBR/CaO

b) XNBR/MgO

c) XNBR/ZnO

Figure 7. SEM images of XNBR vulcanisates

satisfactory, especially in the case of the vulcanisates containing MgO and ZnO (TS_{shr}, EB_{shr} in Table 3).

3.2. Thermo-shrinkable HNBR vulcanisates

3.2.1. Crosslink density and ionic crosslink content for HNBR vulcanisates

Studies performed on the XNBR elastomer crosslinked with nanosized metal oxides confirmed the existence of a biphasic structure and the presence of ionic crosslinks in the elastomer network, which are able to rearrange or decompose upon heating to produce thermo-shrinkable vulcanisates. Therefore, to obtain thermo-shrinkable vulcanisates from the HNBR elastomer, multifunctional crosslinking coagents based on nanosized calcium and magnesium oxides were used in combination with unsaturated carboxylic acids (UCAs). UCAs containing easily abstractable hydrogen atoms and readily accessible double bonds were grafted onto the powder surface during the modification process. Because of their multifunctionality, this type of coagent based on zinc oxide was proven to be able to react

directly with the elastomer and form effective covalent bonds. Moreover, they can form ionic crosslinks that increase the vulcanisate crosslink density and improve tensile strength (Przybyszewska & Zaborski, 2009). Because the presence of ionic crosslinks is crucial for the thermo-shrinkability of vulcanisates, the effect of these coagents on the crosslink density of the vulcanisates and their ionic crosslink content was studied. These results are given in Figs. 8 and 9.

The application of coagents based on nanosized CaO and MgO grafted with UCA caused the formation of ionic crosslinks in the elastomer network. The greatest content of ionic crosslinks was obtained for vulcanisates containing nanosized CaO in combination with oleic and linoleic acid, as well as for MgO with itaconic and linoleic acid. The results of these studies confirmed that these coagents contributed to the increased vulcanisation efficiency. The ionic crosslink content should affect the thermo-shrinkability of the vulcanisates considerably. The crosslinked points in the elastomer network are believed to serve as memory points, enhancing the heat shrinkability.

To confirm that the decomposition and/or rearrangement of the ionic crosslink aggregates is one of the causes of heat shrinkability in the examined HNBR vulcanisates, the crosslink density and ionic crosslink content were determined for the vulcanisates after thermal shrinking and compared with the values of the vulcanisates before thermal treatment.

The data presented in Figs. 8 and 9 suggest that the ionic crosslinks that decomposed during the shrinking of vulcanisates at 70°C allowed the samples to return to their original shape. As a result of the ionic crosslink decomposition, the crosslink density of the vulcanisates decreased. The most considerable reduction of the ionic crosslink number after shrinkage above the ionic transition temperature was observed for the vulcanisates containing CaO-OA, CaO-LA, MgO-IA and MgO-OA as coagents, which were characterised by the highest ionic crosslink content before the heat treatment. These vulcanisates may be expected to show the greatest thermal shrinkage and shape recovery.

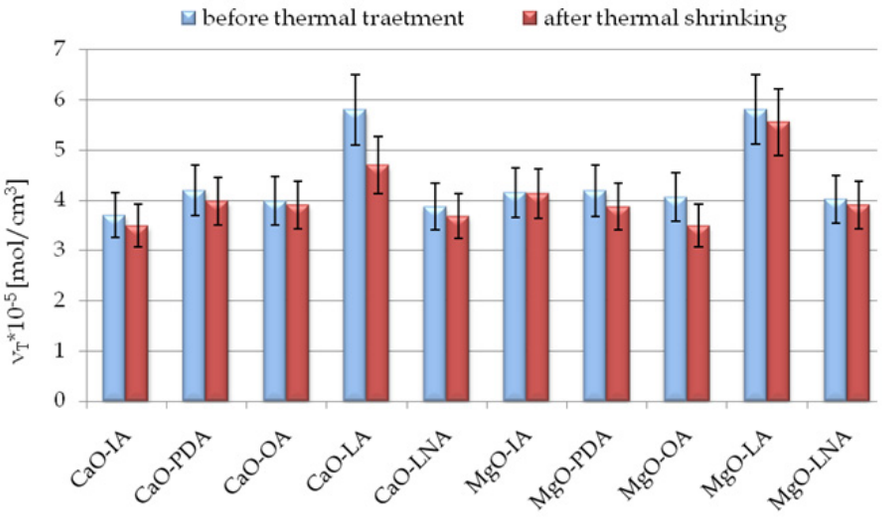

Figure 8. Crosslink density of HNBR vulcanisates

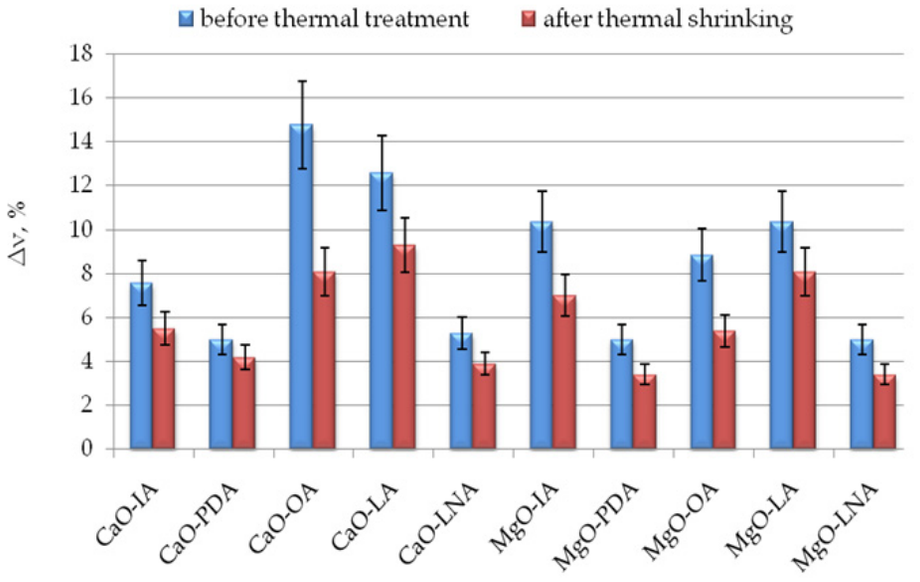

Figure 9. Ionic crosslink content of HNBR vulcanisates

3.2.2. Thermo-shrinkability of HNBR vulcanisates

As mentioned before, the shrinkage of polymer is caused by an internal rearrangement of the structural elements within the stretched sample (Mishra et al., 2000). In contrast to the covalent crosslinks formed during conventional vulcanisation with peroxides, ionic crosslinks are multifunctional and labile. Ionic crosslinks group together, forming clusters that are immersed in the elastomer matrix. Moreover, ionic clusters can rearrange in the elastomer matrix upon external deformation or temperature change.

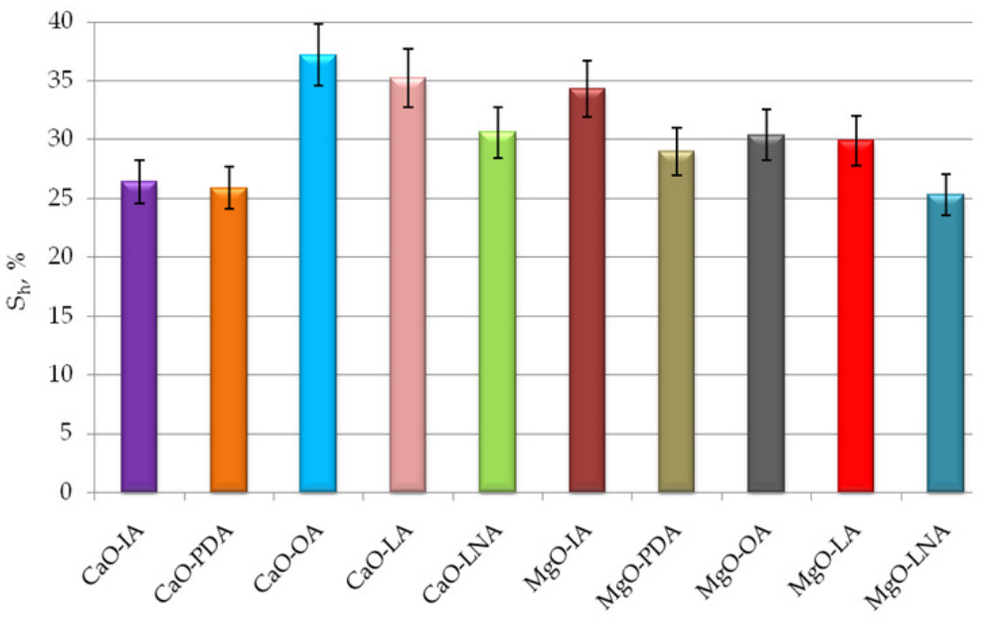

Figure 10. Percentage thermo-shrinkability of HNBR vulcanisates

The crosslinked samples were heated and stretched at 100°C (a temperature above the glass transition temperature). Cooling these samples in this stretched state stabilised the temporary shape. Finally, the stretched samples were allowed to shrink above the ionic transition temperature at 70°C. The heat shrinkability values and percentage recovery of the HNBR samples containing 7 phr of the coagents are presented in Figs. 10 and 11.

The vulcanisates of the HNBR elastomers crosslinked in the presence of coagents based on nanosized CaO and MgO in combination with unsaturated carboxylic acids exhibited heat shrinkability. The greatest shrinkage upon heating (approximately 35%) was achieved for vulcanisates containing the CaO-OA, CaO-LA and MgO-IA coagents (Fig. 10). The lower shrinkability of the vulcanisates with other coagents is a result of the lower crosslink density and ionic crosslink number in their elastomer networks (see Figs. 8 and 9). Because the crosslinked points in the elastomer network serve as shape memory sites, a higher crosslink density improves the shrinkability of the vulcanisate.

The HNBR-based vulcanisates demonstrated good shape recovery performance, with a shape recovery percentage in the range of 91-100% (Fig. 11). The greatest percentage recovery was obtained for the vulcanisates with the highest ionic crosslink content. Moreover, the most considerable reduction of the ionic crosslink number during the thermal shrinking process was observed for these vulcanisates. This result confirms the assumption that the decomposition of ionic crosslinks is the most important reason for the shrinkability and shape recovery of HNBR vulcanisates. It can be concluded that the ionic crosslinks formed in the elastomer by the coagents serve as memory points in the elastomer network.

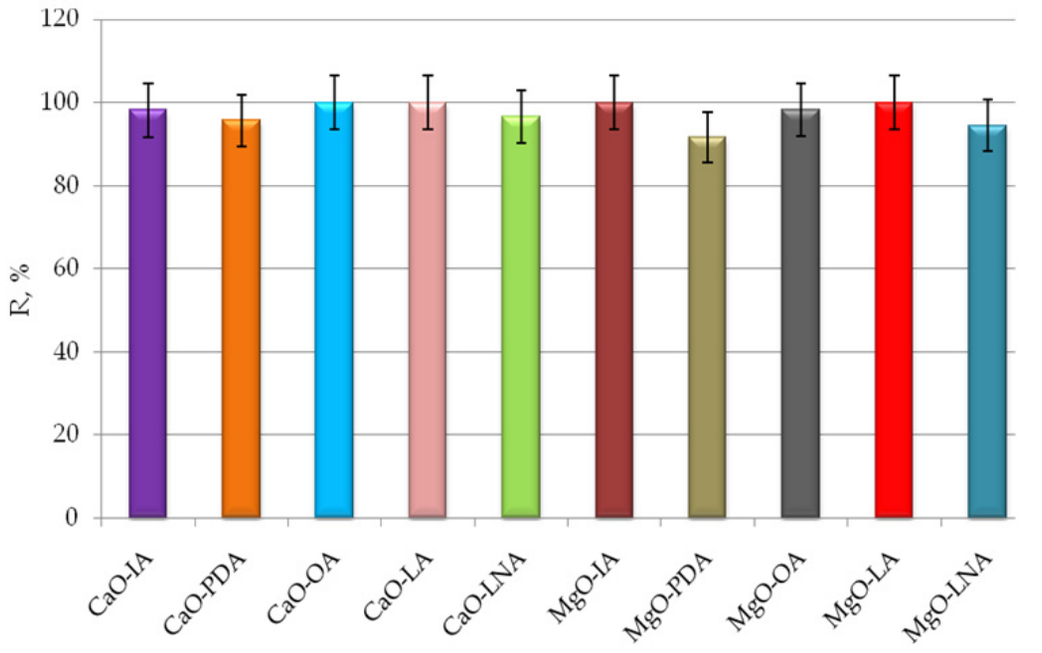

Figure 11. Percentage recovery of HNBR vulcanisates

3.2.3. Dynamic mechanical properties of HNBR vulcanisates

Dynamic - mechanical analysis was performed to confirm the existence of ionic clusters in the elastomer network. The loss factor (tanδ) of the HNBR vulcanisates with coagents is presented as a function of temperature in Figs. 12 and 13 as an example. The values of the glass transition temperature (T_g) are given in Table 4.

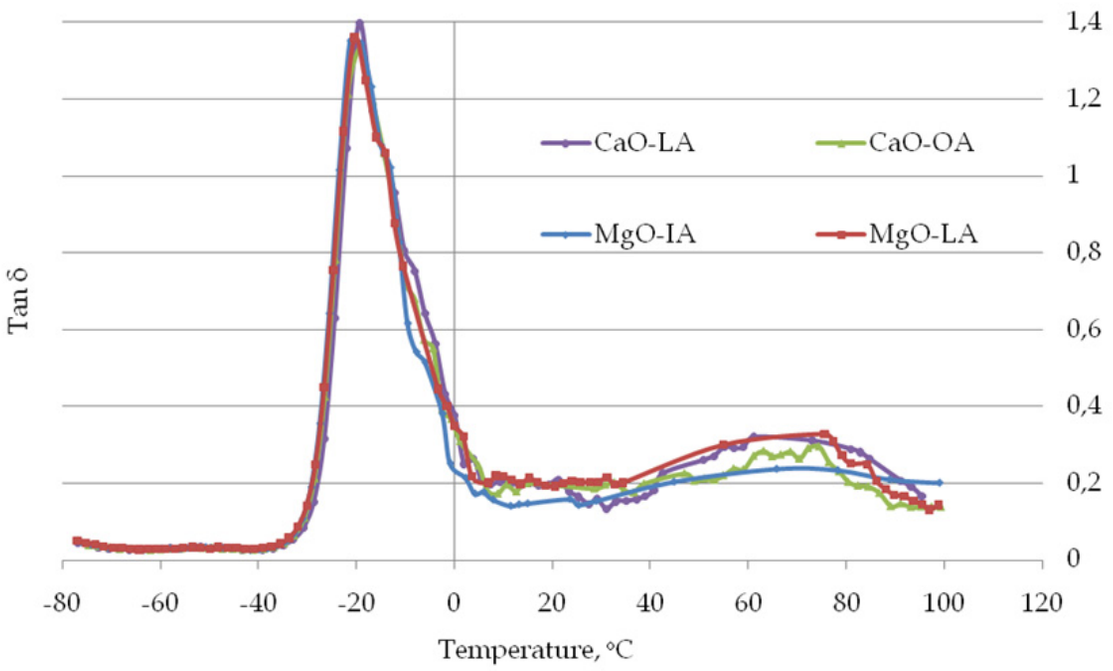

Figure 12. Tan δ versus temperature for HNBR vulcanisates before thermal treatment

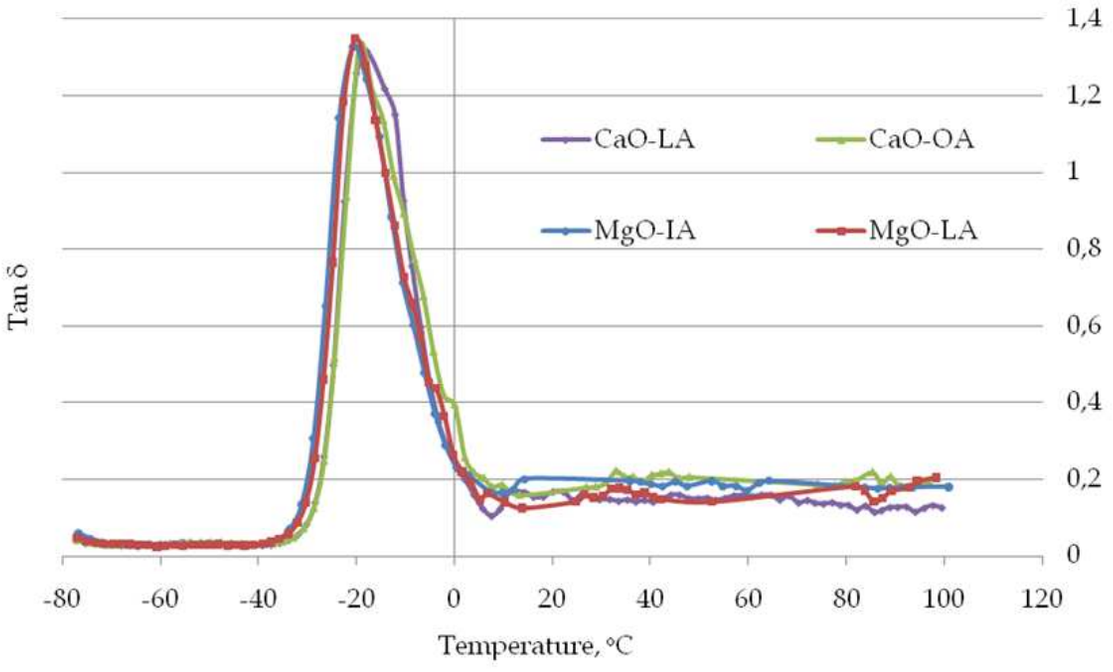

Figure 13. Tan δ versus temperature for HNBR vulcanisates after thermal shrinking

Vulcanisate	T_g before thermal treatment, °C	T_g after thermal shrinking, °C
CaO-IA	-21.2	-22.5
CaO-PDA	-20.7	-21.3
CaO-OA	-20.4	-22.7
CaO-LA	-19.1	-22.0
CaO-LNA	-19.6	-20.8
MgO-IA	-19.4	-22.9
MgO-PDA	-20.3	-21.5
MgO-OA	-20.6	-23.1
MgO-LA	-17.8	-20.4
MgO-LNA	-19.3	-21.0

Table 4. Glass transition temperature of HNBR vulcanisates

The DMA analysis revealed the biphasic structure of the HNBR crosslinked in the presence of coagents based on nanosized CaO and MgO grafted with UCA. Two phase transitions were observed. The glass transition of the HNBR, which occurs at T_g, was observed in the range from (-21.2°C) to (-19.1°C) for vulcanisates with CaO and from (-20,6°C) to (-17.8°C) for vulcanisates containing MgO. The determined T_g values were correlated with the crosslink density of the vulcanisates. A fuzzy low-intensity peak was observed in the temperature range of (40-100°C) (corresponding to the ionic transition) because of the occurrence of a hard phase arising from the existence of the ionic aggregates.

Heating to the ionic transition temperature decreased the glass transition temperature of the vulcanisates by decomposing ionic crosslinks, reducing the crosslink density of the vulcanisates. The greatest decrease of the T_g value occurred in the case of the vulcanisates for which the greatest number of ionic crosslinks decomposed during heating (CaO-OA, CaO-LA, MgO-IA, MgO-OA). The fuzzy peak corresponding to the ionic transition disappeared; consequently, it can be concluded that the shape recovery of the HNBR vulcanisates was caused by the decomposition of the ionic crosslinks and changes in the biphasic structure of the crosslinked elastomer, similarly to XNBR.

3.2.4. Mechanical properties of HNBR vulcanisates

Having established the ability of the HNBR vulcanisates to shrink upon exposure to the ionic degradation temperature and return to their original shape, we then examined their mechanical properties.

It is known that the formation of coagent bridges, which are labile ionic crosslinks inside the elastomer network formed during vulcanisation, improved the tensile properties of the vulcanisates (Przybyszewska & Zaborski 2008, 2009). However, it is reasonable to investigate the effect of the heat treatment of the vulcanisates on their mechanical properties.

As could be supposed, the thermal treatment of the vulcanisates during their shrinkage deteriorated their tensile strength as a result of the decomposition of their ionic crosslinks.

Their tensile strength was reduced by 5% to 30% in comparison with that of the vulcanisates before thermal treatment (Fig. 14). The vulcanisates subjected to shrinking at elevated temperature also exhibited a lower elongation at break (Fig. 15).

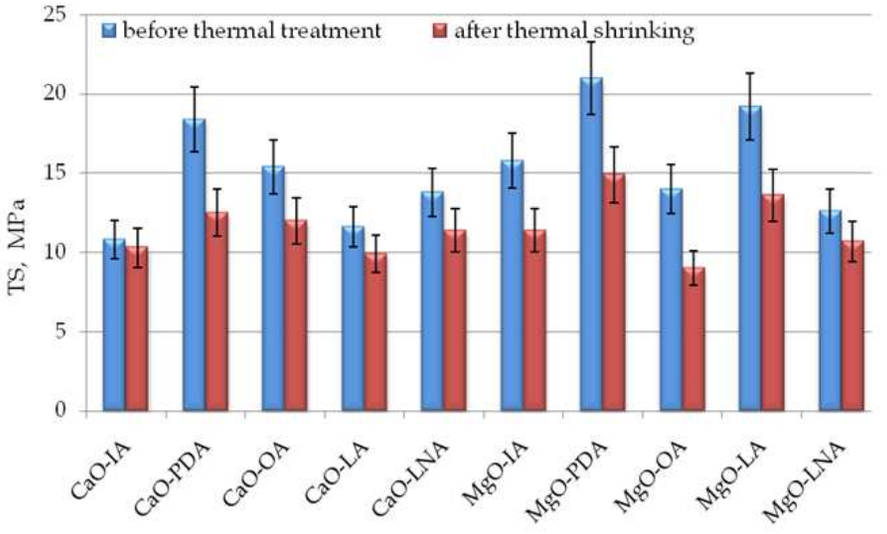

Figure 14. Tensile strength of HNBR vulcanisates

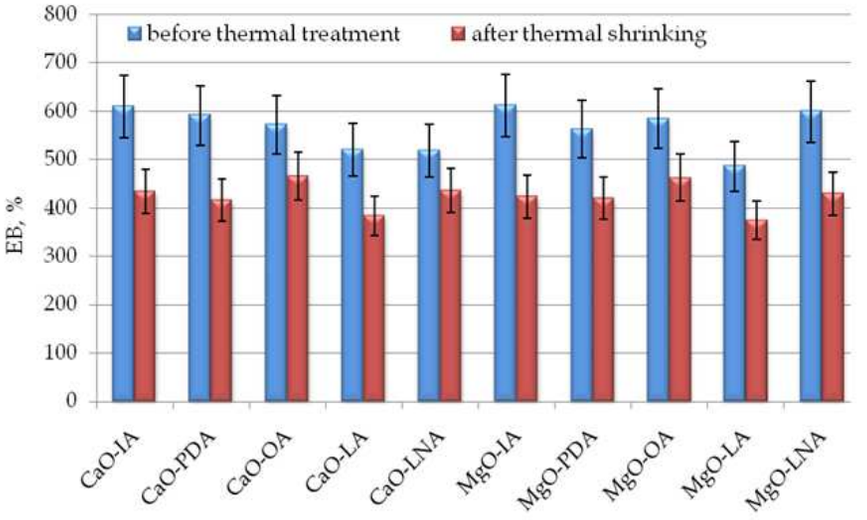

Figure 15. Elongation at break of HNBR vulcanisates

4. Conclusions

The thermo-shrinkable properties of carboxylated (XNBR) and hydrogenated (HNBR) acrylonitrile butadiene elastomer were studied. XNBR was crosslinked with nanosized calcium, magnesium and zinc oxide to ensure the formation of ionic crosslinks in the elastomer matrix, which can serve as memory points and enhance its heat shrinkability. Similarly, HNBR was crosslinked in the presence of coagents based on nanosized calcium

and magnesium oxides grafted with unsaturated carboxylic acids to achieve ionic crosslinks. The examined samples were allowed to shrink at a temperature above the ionic transition temperature. The XNBR vulcanisates revealed thermo-shrinkability in the range of 41% for MgO to 50% for ZnO, whereas the percentage of shape recovery was in the range of 90-100%. Good shape recovery performance was also observed for the HNBR vulcanisates. The greatest shrinkage upon heating (approximately 35%) was achieved for the vulcanisates containing CaO-OA, CaO-LA and MgO-IA coagents. The percentage of shape recovery of these vulcanisates was in the range of 91-100%.

The thermo-shrinkability value and shape recovery ratio were strongly correlated with the ionic crosslink content of the elastomer network, and the number of ionic crosslinks was reduced by heating the samples above their ionic transition temperature. Greater ionic crosslink contents and their more significant decomposition corresponded to vulcanisates with greater thermo-shrinkability. DMA measurements confirmed the presence of ionic crosslinks and the existence of a biphasic structure in both the XNBR and HNBR elastomers. A fuzzy low-intensity peak was observed in the (tan δ) curve, in the temperature range of (50-100^{o}C), which corresponds to the ionic transition that occurs at high temperatures as a result of the occurrence of a hard phase arising from ionic aggregates. This peak disappeared when the samples were heated above their ionic transition temperature. Therefore, it could be concluded that the thermo-shrinkability of the XNBR and HNBR vulcanisates and their shape recovery was a result of the decomposition of ionic crosslinks and changes in or the disappearance of the biphasic structure of the crosslinked elastomer.

Author details

Magdalena Maciejewska and Alicja Krzywania-Kaliszewska
Technical University of Lodz; Institute of Polymer and Dye Technology, Poland

Acknowledgement

The authors wish to acknowledge the Polish Ministry of Science and Higher Education as well as the National Centre of Research and Development for supporting this study.

5. References

Chen, S., Hu, J., Zhuo, H., Zhu, Y. (2008). Two-way shape memory effect in polymer laminates. *Materials Letters*, Vol. 62, No. 25, pp. (4088-4090), ISSN 0167-577X

Flory, P.J., Rehner, J. (1943). Statistical mechanics of cross-linked polymer networks. II. Swelling. *Journal of Chemical Physics*, Vol. 11, No. 11, pp. (521-526), ISSN 1089-7690

Hu, J. (2007). *Shape memory polymers and textiles* (1), Woodhead Publishing Limited, ISBN 978-1-84569-047-2, Cambridge

Ivens, J., Urbanus, M., De Smet, C. (2011). Shape recovery in a thermoset shape memomy polymer and its fabric-reinforced composites. *eXPRESS Polymer Letters*, Vol. 5, No. 3, pp. (254-261), ISSN 1788-618X

Khonakdar, H.A., Jafari, S.H., Rasouli, S., Morshedian, J., Abedini, H. (2007). Investigation and modeling of temperature dependence recovery behavior of shape-memory crosslinked polyethylene. *Macromolecular Theory and Simulation*, Vol. 16, No. 1, pp. (43-52), ISSN 1521-3919

Landlein, A (Ed(s).). (2010). *Shape-Memory Polymers,* Springer, ISBN 978-3-642-12358-0, New York

Leng, J., Du, S. (Ed(s).). (2010). *Shape-Memory Polymers and Multifunctional Composites,* Taylor and Francis Group, ISBN 978-1-4200-9019-2, Boca Raton

Li, J., Viveros, J.A., Wrue, M.H., Anthamatthen, M. (2007). Shape-memory effects in polymer networks containing reversibly associating side-groups. *Advanced Materials*, Vol. 19, No. 19, pp. (2851-2855), ISSN 1521-4095

Mishra, J.K., Kim, I., Chang-Sik, H. (2004). Heat shrinkable behavior and mechanical response of a low-density polyethylene/millable polyurethane/organoclay ternary nanocomposite. *Macromolecular Rapid Communications*, Vol. 25, No. 21, pp. (1851-1855). ISSN 1521-3927

Mishra, J.K., Raychowdhury, S., Das, C.K. (2000). Effect of interchain crosslinking on the shrinkability of the blends consisting of grafted low-density polyethylene and carboxylated nitrile rubber. *Materials Letters*, Vol. 46, No. 4, pp. (212-218), ISSN 0167-577X

Patra, P.K., Das, C.K. (1997). Blends of polyolefins and chlorosulphonated polyethylene (CSM) with special reference to their shrinkability and flame retardancy. *International Journal of Polymeric Materials,* Vol. 35, No. 1-4, pp. (103-118), ISSN 1563-535X

Przybyszewska, M., Zaborski, M. (2008). The effect of zinc oxide nanoparticle morphology on activity in crosslinking of carboxylated nitrile elastomer. *eXPRESS Polymer Letters,* Vol. 3, No. 9, pp. (542-552), ISSN 1788-618X

Przybyszewska, M., Zaborski, M. (2009). New coagents in crosslinking of hydrogenated butadiene-acrylonitrile elastomer based on nanostructured zinc oxide. *Composite Interfaces,* Vol. *16*, No. 2-3, pp. (131-141), ISSN 0927-6440

Ratna, D., Karger-Kocsis, J. (2008). Recent advances in shape memory polymers and composites: A review. *Journal of Materials Science,* Vol. 43, No. 1, pp. (254-269), ISSN 1573-4803

Raychowdhury, S., Mishra, J.K., Das, C.K. (2000). Structure, shrinkability and thermal property correlations of ethylene vinyl acetate (EVA)/carboxylated nitrile rubber (XNBR) polymer blends. *Polymer Degradation and Stability*, Vol. 70, No. 2, pp. (199-204), ISSN 0141-3910

Wang, M., Luo, X., Ma, D. (1998). Dynamic mechanical behavior in the ethylene terephthalate-ethylene oxide copolymer with long soft segment as a shape memory material. *European Polymer Journal,* Vol. 34, No. 1, pp. (1-5), ISSN 0014-3057

Weiss, A., Izzo, E., Mandelbaum, S. (2008). New design of shape memory polymers: mixtures of an elastomeric ionomer and low molar mass fatty acids and their salts. *Macromolecules,* Vol. 41, No. 8, pp. (2978-2980), ISSN 1520-5835

Zhang, H., Wang, H., Zhong, W., Du, Q. (2009). A novel type of shape memory polymer blend and the shape memory mechanism. *Polymer*, Vol. 50, No. 6, pp. (1596-1601), ISSN 0032-3861